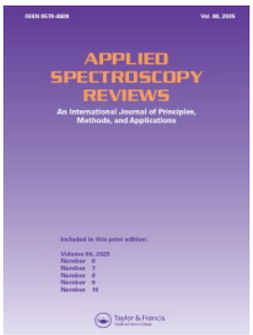

Applied Spectroscopy Reviews

ISSN: 0570-4928 (Print) 1520-569X (Online) Journal homepage: www.tandfonline.com/journals/laps20

# An exhaustive review and experimental exploration of clinical mid-range FTIR urine analysis

Michael Greenop, Amy Crisp, Jessica Barros, Aldo E. E. Segura, Carlos A. Meza Ramirez, Craig Williams, Alison Birtle & Ihtesham Ur Rehman

**To cite this article:** Michael Greenop, Amy Crisp, Jessica Barros, Aldo E. E. Segura, Carlos A. Meza Ramirez, Craig Williams, Alison Birtle & Ihtesham Ur Rehman (13 Aug 2025): An exhaustive review and experimental exploration of clinical mid-range FTIR urine analysis, Applied Spectroscopy Reviews, DOI: 10.1080/05704928.2025.2541109

**To link to this article:** https://doi.org/10.1080/05704928.2025.2541109



Published online: 13 Aug 2025.

APPLIED SPECTROSCOPY REVIEWS
https://doi.org/10.1080/05704928.2025.2541109

Taylor & Francis
Taylor & Francis Group

REVIEW ARTICLE

OPEN ACCESS Check for updates

# An exhaustive review and experimental exploration of clinical mid-range FTIR urine analysis

Michael Greenop[a], Amy Crisp[a], Jessica Barros[b], Aldo E. E. Segura[b], Carlos A. Meza Ramirez[b], Craig Williams[b,c], Alison Birtle[a,d], and Ihtesham Ur Rehman[a,b]

[a]School of Medicine and Dentistry, University of Lancashire, Preston, Lancashire, UK; [b]CCI Photonics, Campus Technology Hub Daresbury Laboratory, Daresbury, Warrington, England; [c]Microbiology Department, Royal Lancaster Infirmary, Lancaster, Lancashire, UK; [d]Rosemere Cancer Centre, Lancashire Teaching Hospitals, Preston, UK

**ABSTRACT**

Urine provides a noninvasive window into the renal and lymphatic systems, providing molecules (potential markers) from around the body that are detectable using mid-range Fourier transform infrared spectroscopy (MR-FTIR). The benefit of MR-FTIR for urine analysis is the simultaneous sampling of many of the 3000+ urine constituents. The highly condensed spectral information in a single drop of urine potentially provides simpler, faster, and cheaper tests for multiple pathologies in a single test, providing hope for simultaneous testing of different pathologies. The shortage of pathologists in the UK and medical experts worldwide motivates research to improve medical diagnostic technologies, increasing interest in techniques like MR-FTIR urine analysis. Clinical MR-FTIR urine analysis is ideally positioned for review, niche enough for an exhaustive progress report, whilst developed enough to highlight challenges and suitable comparison to current approaches. Before clinical spectroscopy can help patients, clinical validation must be demonstrated. The review highlights milestones toward this goal, like replicated or blinded studies. A section is then dedicated to the experimental considerations already investigated, providing a resource for future FTIR urine analysis study design. The paper concludes by testing a critical variable for transmission MR-FTIR spectroscopy, identified by assessment of reviewed references, discussed in only one, urea hydrogen bonding with $H_2O$, emphasizing the importance of robust dehydration protocols for urine MR-FTIR analysis. Academic and industrial collaborators separately duplicated the experiments, increasing confidence in the analysis repeatability and corresponding clinical value of the findings.

**KEYWORDS**

FTIR; clinical; urine; diagnosis; spectropathology; biospectroscopy

**CONTACT** Ihtesham Ur Rehman IURehman@uclan.ac.uk School of Medicine and Dentistry, University of Lancashire, Preston, Lancashire, UK.

## 1. Introduction

Clinical diagnosis using MR-FTIR analysis of urine is a growing area of research. A PubMed database search (Figure 1) shows an early MR-FTIR urine analysis investigating postoperative anuria after thoracotomy in 1966. Interest has grown, with a spike in clinically focused studies in the last decade, the authors decided it beneficial to review progress in the field (Section 2) and highlight key experimental considerations for future studies aiming to push the field forward (Section 3). The investigation covers the related and overlapping fields of biospectroscopy, clinical spectroscopy, and spectro-pathology, resulting in their interchangeable reference in the paper. In reviewing current progress, the authors aimed to draw comparisons to currently available technologies and postulate potential benefits provided by MR-FTIR, alongside developments required for the clinical adoption of biospectroscopy.

A range of reviews and letters have been published about wider biofluid analysis,[1–7] including recommendations for preprocessing[8] and prospects like high throughput[9] or automated disease detection.[10] Interest in the field, enough to justify a Faraday Discussion,[11] explains the increase in MR-FTIR urine analysis literature. The range of MR-FTIR urine analysis applications includes human[12] and bovine[13] doping, detection of microplastics,[14] aerobic exercise assessment,[15] and analysis of dromedary urine added to milk by Bedouins.[16] The versatility of urine analysis is an ideal point of care technology[17] for a range of applications. However, the remit of this review is clinical MR-FTIR urine analysis, allowing discussion of current progress to consider wider context and deeper interrogation of technical considerations.

Aiming to provide a comprehensive review of clinical MR-FTIR urine analysis requires clear inclusion and exclusion criteria. Excluding references where urine is used as a standard,[18] or references focusing on forensic[19–21] applications unless used for protocol refinement useful for clinical studies.[22,23] The authors excluded FTIR analysis of factors isolated from urine, as analyzing of isolates alters spectral interpretation from urine constituent onto bacteria,[24–26] extracellular vesicles,[27] proteins,[28] or extracted/isolated particles.[29–34] Whereas filtered or centrifuged urine samples are included in the filtrate/supernatant (urine fluid component) remains the focus of the MR-FTIR analysis. Focusing the review this way avoids deviating the discussion away from the analysis of urine onto *de facto* cytology, especially where reviews already exist.[35–37]

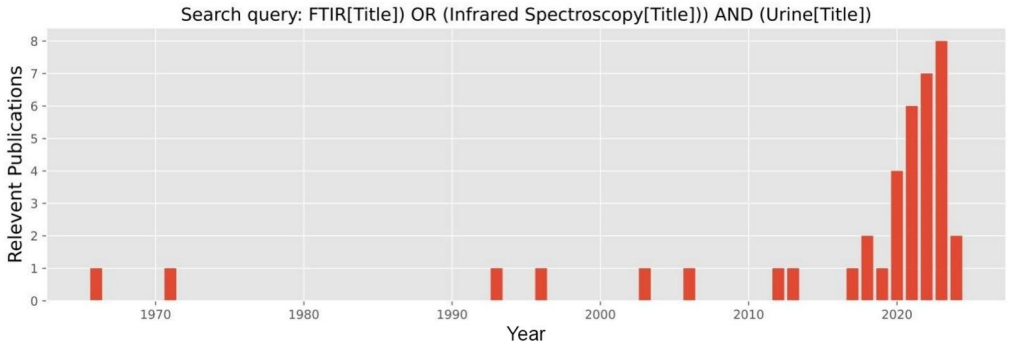


**Figure 1.** Number of FTIR urine analysis publications per year identified using the PubMed search term: ((FTIR[Title]) OR (Infrared Spectroscopy[Title])) AND (Urine[Title]). Figure is author produced.

### 1.1. Inclusion criteria

1. MR-FTIR spectroscopy is applied to a clinically relevant research question.
2. The research question is answered using spectral analysis of urine.

### 1.2. Exclusion criteria

1. FTIR analysis of factors cultured from urine, e.g. bacteria cultured, extracellular vesicles isolated, or particles extracted using centrifuging.

Section 2 is subdivided based on biological transparency, an important consideration for spectropathology using artificial intelligence (AI) with the UK guidelines for AI transparency[38] based on a UK government report.[39] Section 2.1 discusses studies where biological causation is easier to demonstrate. The 3000+ molecular constituents of urine[40] make linking specific biomarkers to diseases complex, albeit desirable to maximize clinical and regulatory confidence. Section 2.2. discusses the breadth of potential targets for MR-FTIR-urine analysis, where pathologies alter urine composition through obscure pathways. Opaque links between identified features and a pathology require increased validation to avoid the concern of overfitting models, typically requiring larger datasets for regulatory approval when increasingly opaque (or black block) AI is employed.[41]

Disease detection, the purpose of clinical spectroscopy, requires regulatory approval and recommendation in medical guidelines (NICE, WHO, etc.) for routine use. Challenges previously highlighted as slowing clinical adoption of biospectroscopy include the protocol consensus and standards required for multi-centre clinical validation.[42–46] Section 3 compares experimental parameters and consistent spectral adaptation relating to experimental variables. The variables are split into pre-experimental controls (Section 3.1), for reference when designing a MR-FTIR urine analysis study.

Section 3.2 outlines experimental variables discussed for reference when designing an MR-FTIR urine analysis protocol. Studies exploring sample variables, like *ex vivo* analysis[22] and freeze-thaw cycles[47] are discussed, aiming to stimulate consensus on a standardized protocol for MR-FTIR sample storage. Variables including sample volume, drying time, and drying temperature are tabulated from the references previously reviewed and compared to studies applying ATR-FTIR. Findings for ATR-FTIR were compared to transmission MR-FTIR experimental results provided by the authors in a repeated analysis between academic (UCLan) and industrial (CCI) partners. The report of duplicated hydration-related alterations in urine MR-FTIR spectra, as compared to spectral adaptations seen in the ATR-FTIR studies.[48]

## 2. Progress in MR-FTIR urine analysis for clinical applications

Compared to molecular techniques like polymerase chain reaction,[49] or proteomics,[50] which identify specific molecules as biomarkers, a broader molecular description is provided by biospectroscopy. Statistical or machine learning (ML) analysis is typically required to link a molecular vibration, or vibrations to a pathology, requiring studies to balance biological interpretability alongside maximizing diagnostic potential. The general composition of urine (Figure 2) reveals that 95% of urine is water, of the remaining 5% there is: urea (40%), phosphate (5.8%) sulfate (4.6%) hippuric acid (2.1%), creatinine

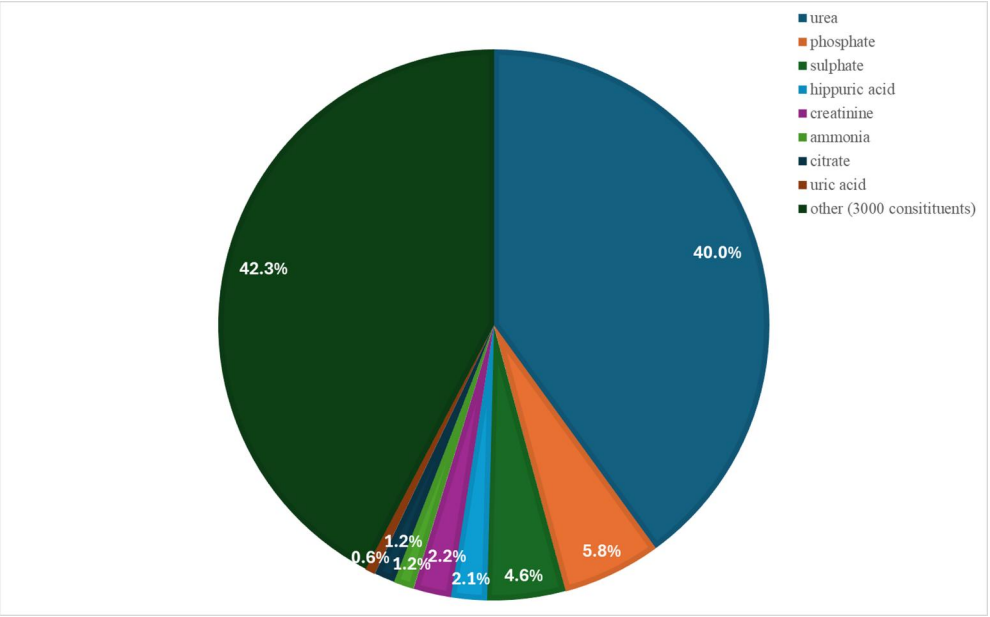


**Figure 2.** Urine is predominantly formed of 95% water. The remaining 5% is composed of the measurable constituents, in the displayed proportions.

(2.2%), ammonia (1.2%), citrate (1.2%), and uric acid (0.6%) are the larger constituents by percentage, with the other near 3000 other constituents taking up the other 42.3%.[40] Highlighting the reality that the isolation of specific molecules in MR-FTIR spectra is unlikely for most urine constituents.

## 2.1. Clear biological link

Examples of direct physical urine-disease contact include Pan et al.[51] and El-Falouji,[52] who looked at urinary tract infections (UTIs) and bladder cancer respectively. Pan et al.,[51] studied 11 controls, and 8 UTI cases. The limited dataset size limited the strength of conclusions, compounded by subdividing UTI cases by infection type, three (*E. Coli*, *P. aeruginosa*, and *E. faecium*) of the four infections only have one sample, with Yeast ($n = 4$). Differences shown in the spectra were related to pathogen type (gram-positive bacteria, gram-negative bacteria, or fungus), with a larger study required to verify and develop the findings.

In a similar study, linking biological evidence to a specific disease, El Falouji et al., investigated FTIR of urine from non-muscle invasive bladder cancer follow-up patients. Their aim was to replace invasive cystoscopy and reduce its associated complications.[52] Of the 62 patients, cystoscopy identified, 41 as cancer-free and 21 recurrences. The identification of a random forest algorithm achieved an AUROC of 92% with 86% sensitivity and 77% specificity. Diagnosis without invasive procedures could be a significant development if FTIR urine analysis were clinically validated.

Currently, diabetes is a key focus for developing similar FTIR-based diagnostics.

### 2.1.1. Diabetes

Studies into MR-FTIR detection of diabetes in urine therefore provide an analytical and hygienic method for abnormal urine-glucose quantification. Two studies developing FTIR for diabetes detection used streptozotocin induction of diabetes in Wistar rats as a model. Caixeta et al.[53] induced diabetes in 18/26 subject rats, of which 10 received insulin treatment. The study identified spectral differences between diabetic (D), non-diabetic (ND), and diabetic with insulin (D + I) classes relating to urea (1452 $cm^{-1}$), creatinine (1490 $cm^{-1}$), and C–O and C–O–C stretching in the 900–1200 $cm^{-1}$ carbohydrate region. The 900–1200 $cm^{-1}$ region separated D and ND rats using principal component analysis (PCA) in the first principal component (PC1). Classification using molecules/molecular groups including urea (sensitivity = 100%, specificity = 88.2, AUC = 0.905, $p = 0.0005$), creatinine (sensitivity = 100%, specificity = 88.2, AUC = 0.958, $p = 0.0001$), and glucose (sensitivity = 100%, specificity = 100, AUC = 1, $p = 0.0001$), showed separation of disease state using individual molecules. Farooq et al.[54,55] subsequently carried out a larger Wisar rat diabetes early detection study, collecting a dataset from 149 samples (86 D, 63 NDs). Blood glucose concentration was determined using tail vein blood and reactive strips (using an MCR-ALS model also used by Caixeta et al $R^2 = 0.79$) to determine the diabetic state, defined as hyperglycemic (>250 mg/dL) 48 h post-injection. PCA-LDA (Linear Discriminant Analysis) models were trained, comparing 2D and 3D-PCA-LDA, with the 3D model achieving 100% accuracy, sensitivity, and specificity. Peaks that were used by both Caixeta et al., and Farooq et al. related to the 1075 $cm^{-1}$ peak for glucose (1072 $cm^{-1}$ for Caixeta et al.) and 1460 $cm^{-1}$ for urea (1450 $cm^{-1}$ for Caixeta et al.).[54,55] One repeated feature was the increased glucose region, where both studies showed a prominent difference in the 900–1200 $cm^{-1}$ region between D and ND.

The link between a single specific peak and a pathology (diabetes) is rare in biospectroscopy. The authors are aware of dedicated diabetes monitoring methods, the capacity to portably test urine glucose has been clinically trialed,[56] which increased monitoring frequency when compared to blood glucose monitoring but no reduction of hyperglycemia incidence or life scores.[57,58] Additionally, the WHO recommends HbA1c as a marker, as it provides an 8–12 week average and does not require fasting.[59,60] The benefit of MR-FTIR over single-molecule tests for diabetes detection (and wider clinical challenges) could be the combined information it provides for situations where testing multiple markers in a single process is advantageous.

### 2.1.2. Diabetes-related complications

Biospectroscopy is additionally benefited by the potential ability to monitor related complications simultaneously with glucose levels for diabetes management. In 2022, Lin et al investigated a range of mice biofluids including, plasma, urine, and saliva, to detect diabetic cardiomyopathy,[61] which is initially asymptomatic but linked to 80% of diabetic deaths alongside other cardiovascular complications. Biofluids were collected from twenty-four male T2DM db/db (Lepr db/db) mice and fifteen male non-diabetic wt/wt mice, with 1 µl drops of biofluid dried onto an ATR-FTIR crystal for analysis. The 900–1200 $cm^{-1}$ region was again linked to diabetes samples but the training of genetic algorithm (GA) partial least squares (PLS) regression models suggested MR-FTIR can

highlight myocardial damage. Saliva performed slightly better than urine, $R^2 = 0.967$ and $R^2 = 0.954$ respectively with a final model trained on data from plasma, saliva, and urine combined ($R^2 = 0.98$).

The potential versatility of MR-FTIR urine analysis is reiterated by Richardson et al.[62] who aimed to develop a lower-cost method of diabetic kidney disease (DKD) detection. Centrifuge filtered samples (0.8 µL) were dried onto an MR-FTIR-ATR crystal from a cohort of 22 controls (healthy individuals), and 155 diabetic patients. The diabetic patient samples were separated into the urinary albumin creatinine ratios that indicate severity, normoalbuminuria ($n = 64$), microalbuminuria ($n = 61$), and macroalbuminuria ($n = 30$). Detection of normoalbuminuria would minimize the risk of permanent nephron damage, early-stage renal, and cardiovascular disease, associated with macroalbuminuria. To achieve that goal two classification models were trained, a PLS-DA (sensitivity = 89.7% and specificity = 97.8%) and SVM (Support Vector Machines) discriminant analysis (sensitivity = 97% and specificity = 100%), highlighted as promising performance compared to urinary dipstick (sensitivity and specificity values as low as 33% and 44% respectively). Regression analysis was carried out using PLS-R and SVM-R algorithms, with a prediction PLS-R model trained to predict albumin concentration. Absorbance at 1651, 1540, 1452, and 1394 $cm^{-1}$, linked to albumin, provides a distinct region of absorption compared to the glucose region (900–1200 $cm^{-1}$) and some distinct regions from the diabetic myocardial damage (3334–3315, 3081–3054, 2937–2910, and 1620–1592 $cm^{-1}$).[61]

The distinct regions, or varied peak combinations linked to diabetes (Section 3.1.1.) and the two diabetes-related combinations[61,62] suggest they could provide a combined test for the long-term management of diabetes. Another finding of this section is the possible nascency of this field of research, with only two diabetes-linked diseases studied, further investigation may identify further targets. Subsequent questions can also be raised, as to whether non-diabetic renal disorders can be detected using MR-FTIR urine analysis.

### 2.1.3. Wider renal issues

Diabetes and diabetes-related complications are not the only renal pathologies with interpretable biological MR-FTIR signals. In 2017,[63] Yu et al aimed to improve on the conventional serum creatinine or proteinuria renal disease biomarkers, which are often detected too late for effective therapeutic intervention. The 1545 $cm^{-1}$ absorption band, linked to amide II (peptide bond) in urinary proteins, was identified as increasing with glomerulonephritis severity in mice ($n = 14$), rats ($n = 54$), and humans ($n = 35$), indicating potential as a better marker than proteinuria.

The link between cardiac and renal health was explored by Kurultak et al.,[40] who noted the precursor of chronic kidney disease, hyperfiltration, and cardiac disease. Tight controls were placed on the recruitment of 37 patients, 17 with RHf (hyperfltraters; RHf (+)), and 20 with normal GFR (normofltraters; RHf(−)). Buhas et al identified the prominent constituents of urine (summarised in Figure 2) in a study identifying renal cell carcinoma (RCC) by testing artificial urine, isolated urine components, and artificial urine spiked with urine components.[64] Creatinine was the only component statistically demonstrated to separate urine samples from RCC patients ($n = 49$) and healthy

controls ($n = 39$), however, PCA-LDA and SVM models trained on the data achieved 82 and 75% classification accuracy respectively. The limited size of many studies through Section 2.1, paired (in many cases) with the observable spectra adaptation, demonstrates the potential for MR-FTIR urine analysis of diabetes detection and renal diseases.

Recently, MR-FTIR and ML algorithms, eXtreme Gradient Boosting (XGBoost), SVM, PLS, and artificial neural networks (ANN) were compared for post-operative markers in urine and plasma.[65] Performance of the models varied from 70% area under the curve (AUC) for SVM and PLS, to near 100% AUC (XGBoost), with absorbance differences in urine between the classes including decreases at the 1072, 1347, and 1654 $cm^{-1}$ bands and increased at 1112, 1143, 1447, 3334, and 3420 $cm^{-1}$.

The range of renal disease markers, showing relatively small sample sizes indicates the potential of MR-FTIR for renal analysis. Clinical validation of the highlighted spectral markers, and identification of further markers could provide a quick and simple diagnosis for multiple renal diseases. The complexity of urine spectral analysis means that the technique should not be limited to simply interpretable classifications. Less interpretable links between diseases and urine require stronger evidence, but if clinically validated appropriately could similarly provide tests for diseases that are not currently available.

### 2.2. Statistically linked

Urine, vital for maintaining homeostasis through lymphatic and renal purification, potentially holds molecular insights into a various conditions. As the biological link becomes less manifest, the probability of finding a single disease-related peak becomes less likely. Dismissing MR-FTIR urine analysis due to reduced interpretability may overlook its potential. As shown by Duckworth et al,[66] which aimed to develop a screening method for pancreatic cancer, incentivized by the <10% 5-year survival rate in the UK resulting from the late-stage manifestation of symptoms (e.g. abdominal pain and jaundice). A small sample size reduced the required resources, with a focus on 'statistical precision' from 'measurement precision' when comparing serum and urine. A patient cohort was recruited and broken into four classes: early cancer ($n = 13$), late-stage cancer ($n = 18$), benign ($n = 30$), and control ($n = 12$). Filters allowed investigation into the ideal particle size ranges for both serum and urine, a potentially beneficial processing step for MR-FTIR spectroscopy in transmission mode, previously shown to suffer from Mie scattering distortions in cell and tissue analysis.[67]

The unfiltered urine was best within the urine analysis samples (accuracy = 86%), with lower accuracy than the highest-scoring serum samples (94%). A detailed breakdown of what constituted benign, and control was provided in the Supplementary Information, allowing differences between model performance when separating a 'related disease'. The leave-one out cross-validation showed a drop in SVM performance between the cancer vs healthy (95%) and cancer vs premalignant (90%). It should be said that the application of spectroscopy for cancer identification, with supplementary testing to identify specific stages or subtypes has been suggested as a possible strategy for the technology. However, it is commendable to highlight the difference at an early

stage of development, along with the recommendation for a larger study over multiple centers for the results to be validated.[66]

### 2.2.1. Gynecology

Along with diabetes and renal studies, gynaecological oncology is a clear focus of interest in the MR-FTIR urine analysis literature. A group from Lancashire, UK provided a series of papers investigating ovarian and endometrial cancers, starting with a pilot study of ($n = 10$) endometrial ($n = 10$), ovarian ($n = 10$), and controls ($n = 10$). The paper highlighted the potential of MR-FTIR analysis of urine as a cost-effective and noninvasive screening and diagnosis technique for gynaecological carcinomas,[68] resulting in larger follow-up studies.[69,70]

The first follow-up study in 2021 focused on ovarian cancer and compared urine, serum, and plasma analysis of patients with ovarian cancer ($n = 116$) and benign ovarian conditions ($n = 307$).[69] Ovarian cancer samples were also investigated for differences between no previous chemotherapy ($n = 71$) and neo-adjuvant chemotherapy ($n = 45$), incentivizing the separation of the groups for comparison with benign controls. The models trained on the different biofluids were assessed using blind predictive models, providing exciting potential for a clinical trial. Assessment again found serum achieving the best performance (sensitivity = 76% and specificity = 98%), with urine reported as performing poorly (sensitivity = 29% and specificity = 87%), looking at the neo-chemotherapy subset. However, the performance between urine and serum more closely matched for the chemotherapy subset: sensitivity = 57% and specificity = 96% (serum) and sensitivity = 57% and specificity = 88% (urine).

A second follow-up paper[70] focused on endometrial cancer. The paper addressed the exclusion of the pilot study[68] from a review,[71] due to the small sample size by increasing the patient cohort. Samples from 219 patients, with the aim of separating endometrial cancer ($n = 109$) and benign genealogical conditions ($n = 110$). An orthogonal projection of latent structures-partial least squares-discriminant analysis model was reported as having sensitivity = 98% and specificity = 97%, significantly higher than the blinded urine analysis for detection of ovarian cancer. Potentially confounding factors that increase the risk of endometrial cancer, Age, BMI, and Diabetes, were tested to determine their effect on the analysis, finding only age with statical significance and none that altered the clustering results.

### 2.2.2. Esophageal cancer

The potential of MR-FTIR urine (and wider biofluid) analysis has been indicated in studies investigating pathologies with physiological separation between the biofluid and disease site. The physical distance between urine production and the esophagus provides an interesting investigation. Do detectable factors travel through the lymphatic, renal, and/or digestive systems?

Or does a systematic physiological adaptation result in esophageal cancer identification in urine? A study exploring the capacity of MR-FTIR to detect esophageal cancer (OAC) in biofluids, including urine[72] trained three models on samples from 127 patients. Spectra were collected from 10 different positions of a dried sample using

ATR-FTIR, analyzing the spectra in the fingerprint (1800–900 $cm^{-1}$ region), with models also trained using saliva ($n = 127$), serum ($n = 124$), plasma ($n = 120$) samples. The challenges of detecting OAC were highlighted, with the samples separated into classes based on the range of confounding stages for OAC including normal ($n = 38$), inflammatory ($n = 19$), Barrett's disease ($n = 27$), low-grade dysplasia (LGD, $n = 6$), high-grade dysplasia (HGD, $n = 11$), and OAC ($n = 25$). The Kennard-Stone algorithm was then used to break the classes into train (60%), validation (20%), and prediction (20%) datasets.

Unlike ovarian cancer, collected using the same equipment and method,[69] the urine provided the highest scores (100% accuracy and following metrics for all classes) for a principal component analysis-quadratic discriminant analysis (PCA-QDA) model trained using the first seven principal components. Additional approaches for feature selection were also applied including genetic algorithm-QDA (GA-QDA) and successive projections algorithm-QDA (SPA-QDA) were used to identify wavenumbers, providing the advantage of highlighting potential specific biomarkers, with the disadvantage of a reduction in reported performance, although with small sample counts per class, a reduction in performance may indicate an avoidance of over-fitting. For some of the smaller classes like HGD and LGD, accuracies for the SPA-QDA (LGD = 96.2% and HGD = 92.6%) and GA-QDA (LGD = 92.6% and HGD = 96.3%) are only possible from prediction datasets of 2 samples (LGD) and 3 samples (HGD) when replicates from the same sample are misclassified, suggesting the need for an optimized protocol to avoid misclassification relating to spectral collection position. Possibly due to sample heterogeneity, an issue repeated throughout much of the existing studies.

## 3. Experimental design considerations

The applications in the previous section demonstrate the progress being made toward clinical application of MR-FTIR urine analysis, with applications including cancer diagnosis,[27,68,70] diabetes monitoring,[54,55] and forensic purposes.[23] The advances demonstrated through Section 2 raise questions around what information must be incorporated into subsequent studies and if there are gaps to bridge. The rise in urine biospectroscopy research has resulted in the publication of useful information regarding experimental variables, currently dispersed over primary articles. The considerable variability across published papers concerning exclusion criteria, sample handling/processing, and different methods of data processing will be compared in this section. The purpose of collating the reported experimental variables through the sections is to assist researchers in implementing suitable and evidence-based experimental design, thereby highlighting a key consideration underreported in current MR-FTIR urine research; variables relating to the dehydration of urine.

### 3.1. Urine composition and pre-experimental considerations

The complexity of urine is indicated in studies reporting spectral variation due to gender, age, medication, time of urine donation, and stream section (early, mid, or late).[73,74] Once water is removed, urine is composed of 8 predominant molecules, and

3000 lower concentration constituents (breakdown of the composition given in Figure 2).[40,75,76] Shared functional groups and similar chemical structures of these molecular groups result in overlapping spectral regions that limit the isolation of specific molecules unless they represent a large proportion of the molecular composition, incentivizing the investigation of key spectral contributions. One approach has been to develop artificial urine, where the largest constituents (by percentage) are altered and the spectral response determined.

### 3.1.1. Urine composition

The main urine feature described in MR-FTIR studies is the dominant urea signal in the infrared spectrum, which hinders the identification of other urine components directly from the spectrum. To overcome this issue, some strategies have been applied including mathematical processing like second-order derivates methods,[47,77–79] urea peak normalization,[77–79] and the use of artificial urine (also used by Pradhane et al.[80]) enriched with urea.[77] Several studies have provided the IR spectra profile of urine components. The peaks associated with the main components of urine along with hydration effected peaks in MR-FTIR studies are shown in Table 1 (Section 3.2.3).

A thorough characterization of urine components was conducted by Sarigul et al. (2021)[79] who analyzed urine samples from both healthy adults and children to establish a reference database of infrared spectra for human urine. The study identified the main aspects of urine spectra, highlighting the dominant urea signal in the infrared spectrum. The main peaks associated with urea were identified at 3420, 3334, 1609, 1447, and 1143 $cm^{-1}$. Spectra saturation is particularly affected by urea signal in the high wave number region (between 3600 and 2600 $cm^{-1}$), however uric acid and creatinine also contribute to specific peaks within this range. Creatinine is also linked to peaks at 1345 and 1238 $cm^{-1}$ while uric acid can be detected by increased absorbance in the regions of 2600–3000 $cm^{-1}$ and 850–650 $cm^{-1}$.

In a study to establish a new artificial urine protocol, the IR spectra of urine collected from 28 healthy individuals were analyzed and compared to three artificial urine formulations.[77] To identify the characteristic peaks of relevant urine components, the spectra of nine urine compounds were also evaluated. The results demonstrated that human urine has a similar spectra profile in the 1800–1200 $cm^{-1}$ region, but significant differences were found within the 1200–800 $cm^{-1}$ range, more specifically at 1644, 1574, 1436, 1105, and 1065 $cm^{-1}$ peaks. Comparing the spectra allowed for the assignment of peaks to human urine components like creatinine, citrate, urea, phosphate, and uric acid. The spectra of artificial urine formulations exhibit considerable similarity with human urine, particularly in the higher frequency region (4000–2500 $cm^{-1}$), with minor discrepancies attributed to distinct urea concentrations in artificial urine formulations. Significant variations were found in the 1200–800 $cm^{-1}$ region, with the most prominent difference around the 975 $cm^{-1}$ position. This spectral region is associated with urea, uric acid, creatinine, and sodium phosphate. Therefore, the results reported, and the fact that artificial urines contain only a small number of the wide range of urine components indicates that the IR spectral profile of urine is dictated by its main components and minor fluctuations in those generate distinct spectral profiles.

**Table 1.** MR-FTIR peak assignments, focused on the information dense fingerprint region of the spectrum, for prominent urine constituents, with reference to hydration and age-linked peak shifts/alterations.

| Wavenumber ($cm^{-1}$) | Vibration | Molecule |
|---|---|---|
| 1658/1657 | H–O–H scissoring<br>C=O stretching (Amide I)<br>C=N stretching (Amide I) | $H_2O$, urea, uric acid, creatinine, & proteins[79]<br>Urea & creatinine hydration shift region[22,48]<br>Age related alteration[22] |
| 1637 | H–O–H scissoring<br>C=O stretching (Amide I) | H2O, urea, uric acid, creatinine, & proteins (alters during dehydration[22])<br>Urea & creatinine hydration shift region[48] |
| 1623 | H–O–H scissoring<br>C=O stretching (Amide I) | H2O, urea, uric acid, creatinine, & proteins (alters during dehydration[22])<br>Urea & creatinine hydration shift region[48] |
| 1609 | N–H deformation<br>C–N–H vibrations | Urea[79]<br>Urea & creatinine hydration shift region[48] |
| 1456 | Asymmetric C–N stretching | Urea[22]<br>Urea hydration shift region[48] |
| 1447 | C–H bending | Urea, uric acid, & creatinine[79]<br>Urea hydration shift region[48] |
| 1345 | C–N stretching | Uric acid & creatinine[79]<br>Creatinine hydration shift region[48] |
| 1238 | C–N stretching<br>$CH_2$ rocking | Creatinine, uric acid, citrate, & sulfate[79]<br>Creatinine hydration shift region[48] |
| 1157 | $NH_2$ deformation | Urea & creatinine hydration shift region[48]<br>Urea, age related alteration[22] |
| 1143 | C–$NH_2$<br>C–O<br>S=O stretching | Urea, uric acid, citrate, & sulfate[79]<br>Urea & creatinine hydration shift region[48] |
| 1113 | C–H<br>C–N–C stretching | Creatinine[79]<br>Creatinine hydration shift region[48] |
| 1081 | $CH_2OH$ groups<br>C–O stretching<br>COH groups<br>$PO_2$—stretching | Symmetric glycosylated proteins/ glycosylated proteins<br>Age related alteration[22]<br>Early sample preparation/creatinine hydration shift[22,48] |
| 1075 | P–O<br>$NH_2$<br>S=O stretching | Urea, sulfate, phosphate, nucleic acids[79]<br>Creatinine hydration shift region[48] |
| 929 | S–O stretching<br>P–OH stretching | Phosphate, sulfate, & nucleic acids[79] |
| 867 | P–OH bending | Phosphate[79] |
| 783 | N–H wagging<br>C–H (ring) bending | Urea & uric acid[79] |

### *3.1.2. Urine controls*

Given that urine components can vary among patients and constitute a significant contribution to MR-FTIR spectra, considerable effort is needed to control factors that could influence these variables. Among the aspects used for patient eligibility criteria, age, and fasting are the most frequently adopted in urine MR-FTIR studies. The effects of age, and gender on the spectra were investigated by the examination of child urine

(3–10 years), young adults (20–30 years), and adults (31–40 years).[79] Results showed that urine spectra from children have fewer variations compared to the other ages. Comparison across the groups shows that sulfate and phosphate groups are impacted by age, as evidenced by differences in 1200–900 $cm^{-1}$ spectra region, more specifically by decreased absorption at 1076 $cm^{-1}$ with increasing age. Gender comparisons reveal that females exhibit slightly higher citrate by differences at 1390 $cm^{-1}$ (despite the age) and demonstrate a higher variance in the region of 1200–1000 $cm^{-1}$ in comparison to men, which is possibly associated with sex-related hormone levels.

While these findings hint at potential effects of age and gender in urine spectra, the PCA analysis was unable to differentiate spectra in both age and gender comparisons but confirmed the results of variance analysis for age-based comparisons. The authors also highlighted that the experiment was conducted with a restricted participant pool, suggesting that further studies are required to make more comprehensive conclusions. Another study also focused on sex discrimination in urine by MR-FTIR, but in the context of forensic application.[23] Urine samples were collected from healthy individual donors within the age group of 20–60 years. The ATR FTIR spectral profiling of male and female urine showed differences in the 1462, 1151, and 1087 $cm^{-1}$ peaks. PLS-DA and PCA-LDA show spectra discrimination between male and female urine with 95.3 and 95.3% accuracy, respectively. However, no significant discrimination was obtained by applying an unsupervised PCA model. Nonetheless, it is important to consider that PCA-LDA must be applied in normally distributed data, which is not reported by the authors in the study and therefore the discrimination might be biased.[81]

Although they constitute only preliminary evidence, these findings suggest the importance of considering age and gender in urine analysis. Typically, MR-FTIR studies discriminate the age range of the participants, even if unspecified as an evaluation criterion. Similar precaution is taken in relation to gender usually the sample group contains a balanced number of female and male human subjects, in a context not involving gender-specific diseases. Fasting is another important consideration to minimize the influence of consumed food, ensuring that urine spectra mostly reflect changes in the metabolism.[77] Overnight or 6h-8h fasting before morning urine samples collection criteria has been adopted in MR-FTIR urine analysis of mammals and humans for diagnosis of diabetes, cancer, autism, and urine components characterization.[40,53,54,61,68,70,77–79]

Apart from being influenced by inter-individual features (like gender, diet, metabolism, and age), the urine composition shows differences throughout the day for the same person.[82] Therefore, a standardized urine collection method is a critical consideration during the experiment design phase. Protocols used previously for urine collection and processing include 24-h and spot urine. 24-h urine collection offers comprehensive information on compounds that fluctuate throughout the day but presents practical challenges for patients and may increase the risk of protein degradation and contamination. In contrast, spot urine collection methods offer greater convenience, standardization, and faster processing and storage.[82] Among single-sample methods, first-morning void provides the least variability in protein concentration and has been reported to have a composition like that of a 24-h collection.[83,84]

Considering that many aspects of the patient can influence MR-FTIR urine spectra, a meticulous selection/exclusion criterion is recommended to control influences on urine composition and maximize the validity and repeatability of studies. Additionally, the choice of specific controls and the patient pools required for a study may vary depending on the pathology or condition under investigation. A good example of a thorough exclusion criteria approach is reported in Sarigul et al., 2023.[78] In their study investigating urine MR-FTIR spectroscopy capacity to detect autism they not only ensured sex, body mass index, and age-matched controls, but also considered patients eating habits and prescribed medicine. The socio-economic situation of the patients and their families was also considered. Interestingly, family income was significantly higher in the controls, revealing how general patient aspects can have an influence on urine composition.

Other studies published by Korkmaz group have been employing tough exclusion criteria for sample selection for urine MR-FTIR analysis. In the work comparing healthy adults and child urine, the list of exclusion criteria included: the detection of leucocytes, protein, blood, glucose, bilirubin and nitrite, urine $5 > pH > 7$, and urinary system complaints.[79] In the study to evaluate renal hyperfiltration, subjects were excluded if presented one of the conditions: acute infection/inflammation, diabetes mellitus, obesity, pregnancy, hypertension, urine albumin $> 30$ mg/day, urine protein $> 300$ mg/day, cardiovascular disease, peripheral artery disease, cerebrovascular disease, chronic rheumatologic disease, and thyroid dysfunction.[40] The exclusion criteria will depend on the study or the research question they aim to answer.

### 3.2. Experimental factors

After effective exclusion criteria definition, it is also crucial to follow adequate procedures of sample handling and processing to ensure the extraction of the maximum information and its accuracy. Given that urine is an unstable biofluid, factors such as sample collection, storage, and preparation time must be carefully observed before analysis.

Sample storage and processing procedures differ among published MR-FTIR research. Figure 3 summarizes some of the most common practices, highlighting that depending on the applied treatment it can impact the interpretability of the results. Additionally, no statistical analysis was used to check spectral differences. Therefore, more investigation on urine storage to check factors like time of storage and freezer/thaw cycles are still required to define experimental aspects for urine analysis.

One of the main experimental variables that can affect spectral stability is the water content in the sample. Water provides a saturation signal that masks peaks in the mid-infrared region, compromising the extraction of biological information. Therefore, proper sample dehydration is typically required before spectral analysis. To counter water masking and ensure sample quality, a range of variables must be considered, see Dehydration on Figure 3. Practicalities also influence sample preparation, relating to the intended application of the technology or the collection mechanism being employed. For example, the application of a point-of-care device may be limited by a requirement

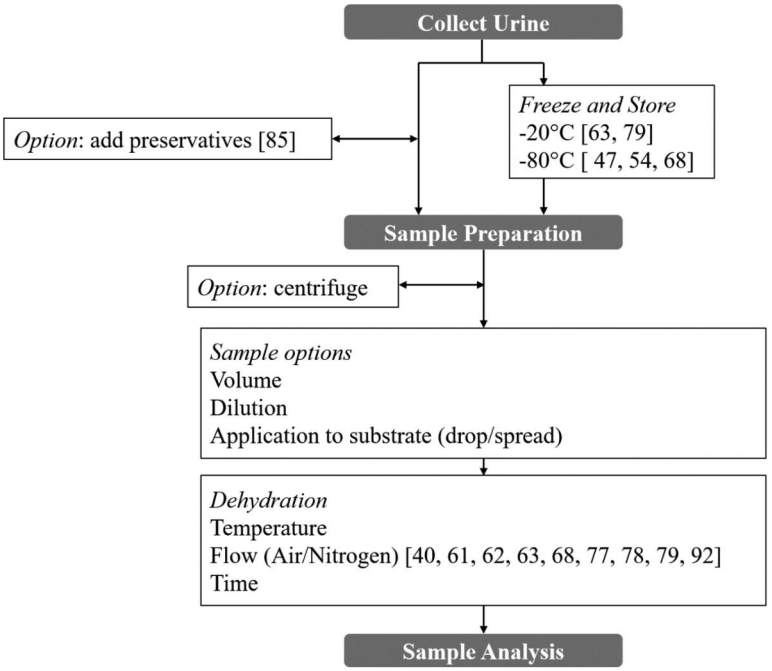


**Figure 3.** Summary of sample processing steps that occur between sample collection and sample analysis that can influence variability in spectral results.

for nitrogen or condensed air. Similarly, transmission and ATR-FTIR provide different advantages, limitations, and sample preparation considerations.

### *3.2.1. Sample preparation*

A sample preparation variable investigated previously is the application of samples onto substrates, focusing on the coffee ring effect.[85] The coffee ring is produced as heavier particles are deposited in patterns relating to the conflicting capillary flow and the Marangoni effect relating to the contact angle between the drop and slide, alongside drying temperate.[86,87] Previous research explored substrate surface adaptation[86,88] inappropriate for FTIR, which requires a consistent surface area. The necessity of a flat surface incentivises the exploration of the most repeatable urine application method.

Consideration of the coffee ring effect is important in ATR- and transmission-FTIR, where the heterogeneous distribution of the sample dried onto substrates reduces variability between spectra collected from the same sample. It is difficult to determine whether a suitable sample cross-section is analyzed when samples are dried directly onto the ATR crystal, an approach employed 11 times in the reviewed literature, along with a flow of nitrogen or air to speed drying. The different approaches also potentially influence sample volume choice, with drying samples directly onto the ATR crystal using $<10\,\mu l$, potentially selected to reduce the drying time and increase the percentage of the sample interacting with the infrared beam during analysis. Samples left on coated slides are frequently left overnight,[23,66,69] allowing the selection of 30–60 µl, potentially selected to improve the sample connection to the crystal during clamping.

In a transmission FTIR context, only one clinical MR-FTIR urine analysis application was found by the authors,[66] limiting the scope for technique comparison. To fill this gap, the authors have provided a comparison (method in supporting material) of techniques discussed for other biofluids applied to urine analysis (method: SI1.4.). Testing the hypothesis, dropping the sample directly onto the substrate produces a more consistent spectrum, was carried out using calcium fluoride ($CaF_2$) slide over two stages, either spreading using a pipette tip or as been used in plasma and serum[89,90] analysis, through dilution of the biofluid.

The first (Figure 4(A,B)) compared dropping, defined as applying the sample directly to the slide without agitation and spreading, where a pipette tip is used to mix the sample over an area. The average spectra and standard deviation for 5 samples are plotted for the smear (black) and drop (red). The larger standard deviation for samples dropped onto the slide suggesting spreading increases spectral repeatability. Figure 4(B) shows the PC1 v PC2 score plot for dropping (red dots) and smeared samples (black dots), revealing a tighter cluster for smeared samples and a larger distance between drop preparations.

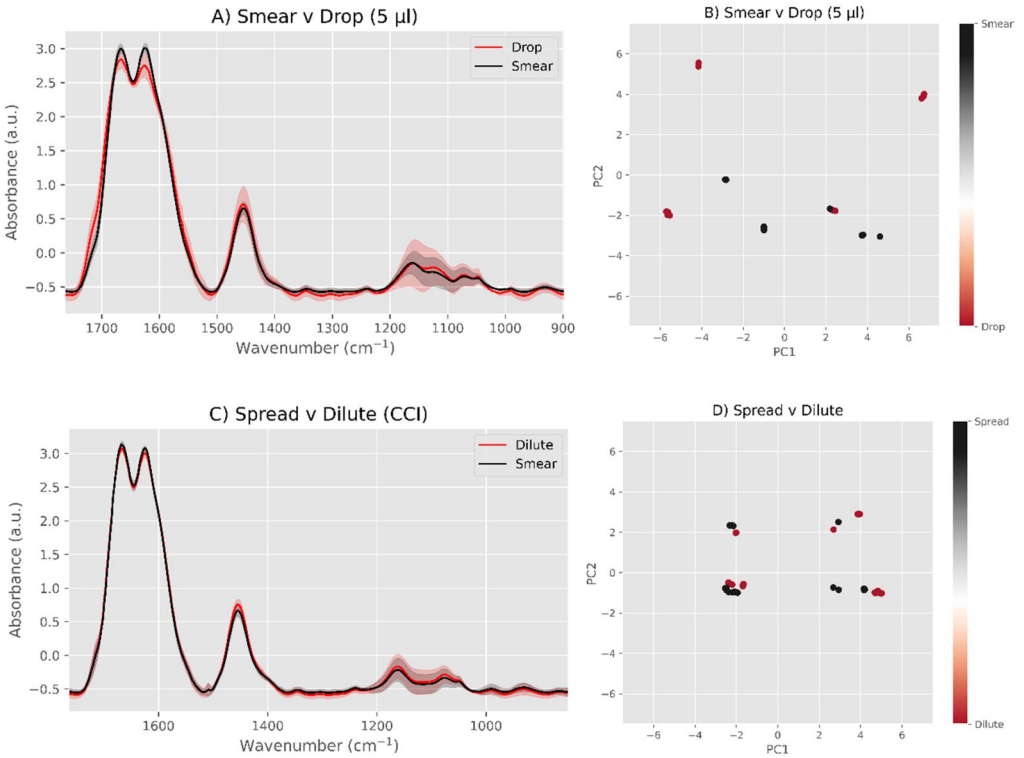


**Figure 4.** (A) Mean spectrum with standard deviation (shading) for samples dropped (red) and smeared (black) onto $CaF_2$ slides. (B) PCA score plot (PC1 v PC2) for samples dropped (red) and smeared (black) onto slides. (C) Mean spectrum with standard deviation (shading) for samples diluted (red) and spread (black) onto slides. (D) PCA score plot (PC1 v PC2) for samples diluted (red) and spread (black) onto slides. Absorbance below zero due to standard normal variate. Figure is author produced.

The increased spectral repeatability (reduced variability) for samples spread over the slide is a similar investigation as carried out previously,[89,90] where serum was diluted using deionized water to reduce drop cracking during dehydration. The dilution of urine samples was hypothesized as an approach for spreading the sample for increased uniformity. The sample would be applied to the slide by cycled (2–3 cycles) dispersion and aspiration (drop) and compared to samples smeared over the slide surface to an approximate 1 cm diameter area (smear). Figure 4(C) shows the mean spectra for five samples prepared using each method, with a more closely matching standard deviation for spread (black) and diluted (red).

The similarity between spreading by pipette aspiration cycling/dilution and pipette tip smearing was reiterated by the overlapping PCA score plot clusters, with groups relating to individual samples rather than application group (Figure 4(D)). Figure 4 suggests with training, inconsistencies in the spreading area do not denigrate MR-FTIR spectral repeatability enough to justify the additional drying time incurred through dilution, as least for transmission spectra collected from the entire sample area. However, the heterogeneous nature of biofluid samples should be a consideration for applications requiring ATR collection from different locations of a biofluid sample or vibrational spectroscopy mapping. Time must be taken to ensure the spectral influence of hydration described in previous papers for urine.[22,48]

### 3.2.3. Warming urine samples in MR-FTIR urine analysis

Different approaches taken to dehydrate urine samples in the literature typically take two routes, temperature, or flow, to speed sample dehydration when drying samples directly onto ATR crystals, reducing drying time but making the technique dependent on the availability of flow supply. Another approach is drying samples onto coated slides,[69,70,72] possibly to avoid the requirement of air/nitrogen flow by allowing the preparation of multiple samples in a single process.

Temperatures are reported as 'room temperature overnight' making precise replication impossible but is better than omitting time and temperature details altogether. Of the references reporting dehydration time, with the range from 2 to 45 min for the samples dried directly onto the ATR crystal. Spectral variability relating to drying time was investigated by Das et al.,[22] who highlighted time-related spectral changes in three biofluids, including urine. Spectra were collected by dropping 50 µl from 4 cm above the ATR crystal and collecting spectra at 2 min intervals. The biofluids were deemed dry once a consistent spectrum was produced over three consecutive intervals. Table 1 tabulates key urine peaks identified by Das et al, highlighting the regions associated with urine (urea/creatine-water interactions) hydration alongside corroborating evidence provided by Oliver et al,[48] and Sarigul et al.[79]

To develop the investigation into the temperature for transmission analysis, the authors carried out a duplicate experiment (method: SI1.5.), repeated in two locations (CCI & UCLan). Five urine samples (5 µl) were smeared onto $CaF_2$ slides and dried using a slide warmer set to 30 °C (full method in Supplementary Information) and MR-FTIR spectra were collected at times 0 min, after 2 more minutes at 30 °C, and then additionally 4, 8, and 10 min at 30 °C. Figure 5 shows the averaged spectra for each time step and wavenumbers indicated by Freidman statistic ($p < 0.0001$) for the

| Time - Freidman ($cm^{-1}$ p<0.0001) | |
|---|---|
| UCLan ($cm^{-1}$) | CCI ($cm^{-1}$) |
| - | 1764-1748 |
| 1705-1679 | 1736-1703 |
| 1668-1612 | 1690-1656 |
| - | 1632 |
| 1600-1592 | 1621-1580 |
| 1504-1415 | 1565-1486 |
| 1384-1369 | 1385-1361 |
| - | 1321-1295 |
| - | 1273-1264 |
| - | 1251-1221 |
| 1208-1176 | 1203-1130 |
| 1127-1094 | - |
| 1047 | 1008-972 |
| 1000-996 | |
| 984-978 | - |
| - | 947-941 |
| - | 908-890 |
| - | 863-849 |

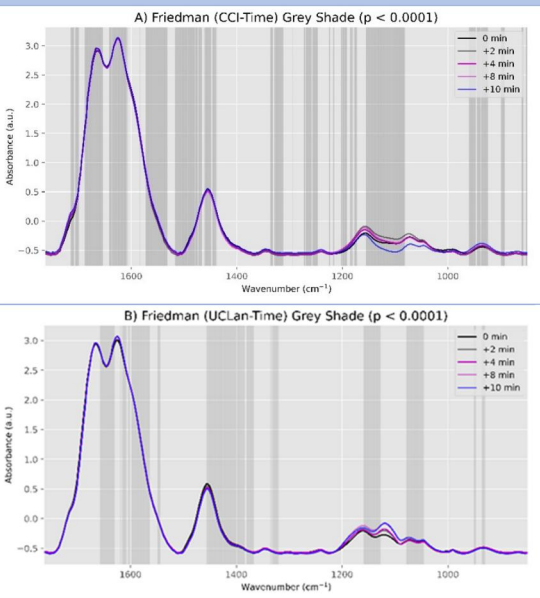


**Figure 5.** Freidman statistic over 0, +2, +4, +8, +10 min for UCLan (A) and CCI (B). Absorbance below zero due to standard normal variate. Figure is author produced.

experiment at CCI (A) and UCLan (B). Several regions were highlighted (Figure 5 – Table) by the Freidman test, which provided several overlapping statistically significant regions including an amide I shoulder (1705–1703 $cm^{-1}$) linked to urea hydration.[48] Amide I regions (1668–1656 $cm^{1}$ & 1592–1580 $cm^{-1}$) and amide II (1504–1486 $cm^{-1}$) were highlighted at CCI and UCLan, alongside 1384–1369, 1203–1176, and 1047 $cm^{-1}$.

Statistically significant regions that were not duplicated demonstrate the value of repeating experiments, especially in different locations to identify aspects of the analysis vulnerable to overinterpretation. Molecular causes of inconsistencies could relate to the complex hydrogen bonding that occurs between $H_2O$ and urine constituents,[48,91] especially urea.[92,93] Varied urea-water interactions are exacerbated when sample thickness and composition cannot be assumed homogeneous, as is the case for MR-FTIR urine analysis. To investigate urea hydration further, Nemenyi *post-hoc* test linked statistical differences to time steps (Table 2).

For CCI, a shrinking range of statistical significance focuses on the amide I peak, starting broader between time 0 and 2 min (1686–1657 $cm^{-1}$), narrowing slightly between 2 and 6 min (1684–1660 $cm^{-1}$), and narrowest at 6–14 min (1670–1660 $cm^{-1}$), related to the removal of $H_2O$ amide I contamination through continued dehydration, with the 1670–1663 $cm^{-1}$ region appearing as significant in the 2–6 min timeframe at UCLan. The uric acid/creatinine linked 1390–1370 $cm^{-1}$ (UCLan) was also repeated (1374–1366 $cm^{-1}$ – CCI) in the 0–2 min timeframe. However, statistically significant differences were not seen past 6 min for UCLan and 14 min for CCI. Total dehydration removed statistical differences from both repeats, aligning with the hypothesis that hydrogen bonding within the urine components, especially urea, caused misalignment of CCI and UCLan replicates. The discrepancy in dehydration time between UCLan

**Table 2.** Nemenyi *post-hoc* ($p < 0.001$) test in over separate time-steps at UCLan and CCI.

| Time – Nemenyi *Post hoc* Test ($cm^{-1}$ – $p < 0.001$) | | | | |
|---|---|---|---|---|
| | Time 0–2 min | 2–6 Min | 6–14 Min | 14–24 Min |
| UCLan ($cm^{-1}$) | **1390–1370** | **1670–1663** | | |
| | 997–995 | **1636–1625** | | |
| | 983 | 1621–1612 | | |
| | | 1590–1586 | | |
| | | 1580–1570 | | |
| | | | | |
| CCI ($cm^{-1}$) | 1760–1750 | **1684–1660** | 1670–1660 | |
| | 1686–1657 | **1620–1530** | 1618–1607 | |
| | 1612–1580 | | | |
| | 1525–1515 | | | |
| | **1374–1366** | | | |
| | 1250–1240 | | | |
| | 1233–1224 | | | |
| | 1200–1190 | | | |
| | 1184–1182 | | | |
| | 1005–1000 | | | |
| | 983–973 | | | |
| | 908–900 | | | |
| | 893–890 | | | |
| | 864–860 | | | |
| | 849 | | | |

Bold = Repeated at both centers and italic = continued over time-steps.

and CCI may result from differences in room temperature but both reduced drying times compared to room-temperature drying of urine, the 20-minute (mean) drying time identified by Das et al.[22]

### 3.2.4. Heat-related FTIR spectral adaption in urine

Using temperature to dehydrate urine samples provides the advantages of reducing sample preparation time (simplifying point-of-care diagnoses) and incentivizing the publication of a specific temperature (improving repeatability). The main concern when using temperature is that a protocol is in place for the safe handling of slides (where appropriate) and sample stability. To investigate sample stability, aiming to identify potential regions of denaturation in the sample (within a reasonable handling temperature range), an experiment was again duplicated between CCI and UCLan (method: SI1.6.). Five samples were again analyzed over increments, with spectra collected when samples (5 µl smeared on $CaF_2$) were dried at 30 °C and again when the samples were exposed to 60 °C and again at 90 °C.

Figure 6 shows the results from UCLan (A) and CCI (B), with the Friedman statistic ($p < 0.0001$) shaded in grey (and tabulated) over the average spectra for each temperature step (30, 60, and 90 °C). Freidman test showed the amide I shoulder 1729–1677 $cm^{-1}$ linked with urea/urea hydration,[48,79] the 1630–1590 $cm^{-1}$ Amide I/II region (urea and creatine hydration,[48] and the O–H peak of water[22]), and the 1200–1105 $cm^{-1}$ related to key urine components (Table 1). The final duplicated region is 1027–982 $cm^{-1}$ phosphate, sulfate, & nucleic acids.[79] Some spectral regions were again not duplicated, indicating the variability of urine samples, alongside the previously stated influence of hydrogen-bonded urea and creatinine.[48]

The repeated analyses identified several unmatched spectral regions (Figure 6) however, key regions were identified for different temperature steps. To investigate the

| Temp - Freidman ($cm^{-1}$ $p<0.0001$) | |
|---|---|
| UCLan ($cm^{-1}$) | CCI ($cm^{-1}$) |
| 1764-1752 | - |
| 1725-1677 | 1729-1707 |
| - | 1664-1656 |
| 1642-1640 | - |
| - | 1615-1611 |
| 1631-1590 | 1602-1591 |
| - | 1569-1567 |
| - | 1558-1527 |
| - | 1514 |
| - | 1498-1481 |
| - | 1465-1401 |
| 1405-1392 | 1376-1369 |
| - | 1248-1244 |
| 1221-1208 | - |
| 1173-1148 | 1200-1105 |
| 1139-1137 | - |
| 992-990 | 1027-982 |
| - | 903-902 |
| - | 890-867 |

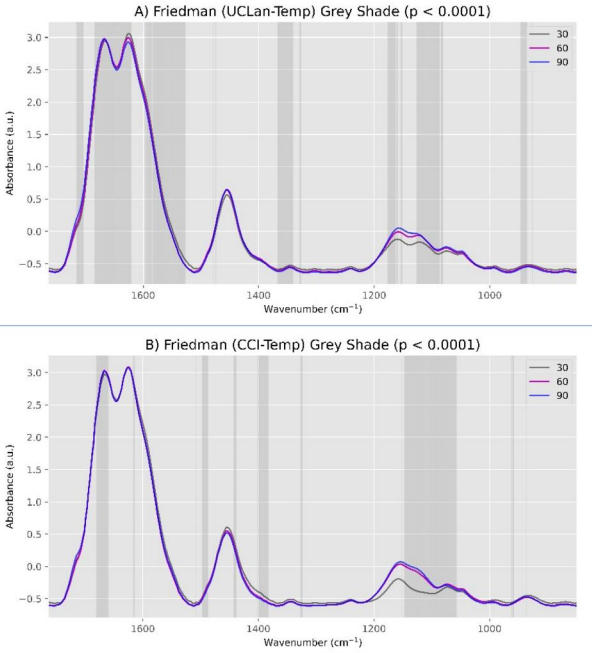


**Figure 6.** Freidman statistic for 30, 60, and 90 °C for CCI (A) and UCLan (B), with table comparing UCLan and CCI analysis Freidnam ($p < 0.0001$) regions, ranges on same row are repeated regions. Absorbance below zero due to standard normal variate. Figure is author produced.

stepwise changes relating to temperature further, Nemenyi *post-hoc* ($p < 0.001$) was carried out (Table S1) on spectral regions indicated by the Freidman test. The key region when comparing 30 and 60 °C is the 1150–1170 $cm^{-1}$, appearing at both UCLan and CCI, similarly replicated was the 1729–1707 $cm^{-1}$ region for the 60–90 °C. The 1150–1170 $cm^{-1}$ region for 30–60 °C is associated with $NH_2$ deformation (urea/hydrated urea/urine age-related degradation[22,48]) highlighted in section 3.2.3, with 1729–1707 $cm^{-1}$ appearing as a slight shoulder on the amide I peak, potentially linked to denaturation of proteins.

Variations between different hydration levels, drying times, and temperatures suggest that the prominence of sample hydration relative to a given research question should be addressed early in an MR-FTIR urine analysis study. A single reference[70] mentioned the amount of time between the donation of the sample and freezing. Consideration of freeze-thaw cycles,[47] dehydration protocol,[48,85] and time *ex vivo*[22] raise the question of whether preservatives should be used or whether their inclusion will introduce new distortions. The abundance of experimental variables and potential provides a fertile research field and incentivises further investigation into sample preparation and wider clinical applications of MR-FTIR urine analysis. Notably, statistically significant regions have been linked to water-urea/water-creatine interactions[48] for the temperature steps (Figure 6) higher temperatures might be possible for applications requiring rapid analysis. However, the key region used for qualitative assessment of sample dehydration (amide I & II), is exactly the spectral region of the denatured proteins, making their isolation complex, and highlighting the need for further research.

## 4. Conclusions and next steps

MR-FTIR provides clinical insights by simultaneously sampling the molecular constituents of urine, without the need for reagents.[94] The potential of the technique was demonstrated in Section 2, with not only diabetes (1072 $cm^{-1}$ – Caixeta et al.[54]) but complications, e.g. diabetic kidney disease detection through albumin (1651, 1540, 1452, and 1394 $cm^{-1}$ – Richardson et al[62]) but wider renal disorders (Section 2.1.3) and diseases indirectly linked to urine (Section 2.2).

The distinct signatures of the different diseases are strong evidence that further development can provide a technique for detecting and monitoring a range of renal and diabetes-related disease pathways in a single cheap, simple, and noninvasive test. However, key markers identified for several diseases are in spectral regions shown to vary relating to urea and creatinine hydration,[48] incentivizing a deeper investigation into urine sample dehydration using transmission MR-FTIR.

The wider molecular context provided by vibrational spectroscopy comes with the cost of complex biological interpretation of urine spectra. Statistical techniques were shown to expand the clinical applications of MR-FTIR urine analysis to gynaecological applications and anatomical regions with obscurer links to urine like the Esophagus. Applying ML/chemometric/multivariate techniques extends the potential for clinical spectroscopy but obscures the association of spectral features to classifications/diagnoses. The thousands of vibrational spectroscopy features (wavenumbers) used to train biospectroscopy algorithms risk overfitting models (forced prediction of classes).

To counter overfit models, which waste time, effort, and funding by failing to generalize to new data, risking the credibility of researchers and the field, blinded and ideally multi-centre studies are imperative. Standardization and multi-centre studies are stated targets for clinical spectroscopy translation.[44,45] No multi-centre or multi-instrument MR-FTIR urine analysis studies were found by the authors. However, blind testing for ovarian cancer is a promising development.[69] Section 3 compiled studies investigating key experimental variables for MR-FTIR urine analysis, comparing findings for ATR, and expanding into transmission. The influence of patient sex,[23] age,[79] and sample storage[47] on spectral composition were described, and the influence of the dehydration temperature and time was demonstrated.

Section 3 extends the review of progress provided in Section 2 by providing a centralized resource for FTIR urine analysis researchers, alongside demonstrating the effect of repeating an analysis with different researchers and locations. Although the repeated experiments were small ($n = 5$ per class), demonstrating reduced $H_2O$ contributions in the 1686–1657 $cm^{-1}$ amide I region as a key urine hydration marker, confirming that 30 °C dehydrates 5 µl of urine in 14 min without sample degradation. Differences were shown between 30, 60, and 90 °C, but changes could not be separated from dehydration-linked changes conclusively, resulting in a current recommendation to avoid speeding up dehydration further by using 60 or 90 °C. However, further investigation is required to identify spectral adaptations that might occur, possibly relating to protein denaturing.

Repeating experiments in two locations A) Requires a strict protocol to be developed, preparing the technique for larger validation studies and eventual regulation, and B) Reduces the risk that over-interpretation or bias in the analysis is inadvertently

published. For example, the repeated analysis focused spectral interpretation onto spectral regions highlighted in both locations, indicating their potential robustness to inter-operator variability. A development on the current protocol is incorporating a standard specific to the analysis being carried out, with one previously investigated option being potassium thiocyanate.[95] The current protocol used the Thermo Fisher Factory Test and qualifications test, which are built into the Summit Pro to meet US, EU, Chinese, and Japanese pharmacopeia standards. However, the implementation of a quicker standard would provide greater comparison between equipment.

By showing differences between measurements of the same sample (Figures 5 and 6) we highlight the inconsistency between preparations using different dehydration times and temperatures. The differences demonstrated in Figures 5 and 6 therefore indicate the kinds of differences that can occur between (and even within) sample preparations of the same sample (intra-sample variability) relating to hydration state. Although the authors acknowledge that simply drying for longer, or at higher temperatures may be seem a simple solution, we have shown that the replication of results required to speed clinical approval of the technique necessitates publication of dehydration routines. We suggest that future research be carried out investigating intra-sample variability in relation to stability of identified biomarkers over repeated experiments.

## Acknowledgment

The authors would like the National Cancer Institute (Dr. Greenop), North West Cancer Research (Dr. Crisp), and Innovate UK (CCI Photonics) for their support.

## Disclosure statement

One paper reviewed (Ramirez et al, 2022[70]) was authored by a coauthor of this paper. No additional conflict of interest is present.

## Funding

This work was supported by National Cancer Institute (Dr. Greenop), North West Cancer Research (Dr. Crisp), and Innovate UK (CCI Photonics) for their support.

## ORCID

Michael Greenop http://orcid.org/0000-0003-4894-7466
Ihtesham Ur Rehman http://orcid.org/0000-0003-2502-7608

## References

1. das Chagas e Silva de Carvalho, L. F.; de Lima Morais, T. M.; Nogueira, M. S. *Providing Potential Solutions by Using FT-IR Spectroscopy for Biofluid Analysis: Clinical Impact of Optical Screening and Diagnostic Tests*; Photodiagnosis Photodyn Ther., **2023**, December 1.
2. Aitekenov, S.; Sultangaziyev, A.; Abdirova, P.; Yussupova, L.; Gaipov, A.; Utegulov, Z; Bukasov, R.. *Raman, Infrared and Brillouin Spectroscopies of Biofluids for Medical Diagnostics and for Detection of Biomarkers*; Crit. Rev. Anal. Chem., **2023**.

3. Sala, A.; Anderson, D. J.; Brennan, P. M.; Butler, H. J.; Cameron, J. M.; Jenkinson, M. D.; Rinaldi, C.; Theakstone, A. G.; Baker, M. J. *Biofluid Diagnostics by FTIR Spectroscopy: A Platform Technology for Cancer Detection*; Cancer Lett., **2020**, May 1.
4. Theakstone, A. G.; Rinaldi, C.; Butler, H. J.; Cameron, J. M.; Confield, L. R.; Rutherford, S. H.; Sala, A.; Sangamnerkar, S.; Baker, M. J. Fourier-Transform Infrared Spectroscopy of Biofluids: A Practical Approach. *Transl. Biophotonics*. **2021**, *3*, 1–20. DOI: 10.1002/tbio.202000025.
5. Baker, M. J.; Trevisan, J.; Bassan, P.; Bhargava, R.; Butler, H. J.; Dorling, K. M.; Fielden, P. R.; Fogarty, S. W.; Fullwood, N. J.; Heys, K. A.; et al. Using Fourier Transform IR Spectroscopy to Analyze Biological Materials. *Nat. Protoc.* **2014**, *9*, 1771–1791. DOI: 10.1038/nprot.2014.110.
6. Baker, M. J.; Hussain, S. R.; Lovergne, L.; Untereiner, V.; Hughes, C.; Lukaszewski, R. A.; Thiéfin, G.; Sockalingum, G. D. Developing and Understanding Biofluid Vibrational Spectroscopy: A Critical Review. *Chem. Soc. Rev.* **2016**, *45*, 1803–1818. DOI: 10.1039/c5cs00585j.
7. Leal, L. B.; Nogueira, M. S.; Canevari, R. A.; Carvalho, L. F. C. S. *Vibration Spectroscopy and Body Biofluids: Literature Review for Clinical Applications*; Photodiagnosis Photodyn Ther., **2018**.
8. Butler, H. J.; Smith, B. R.; Fritzsch, R.; Radhakrishnan, P.; Palmer, D. S.; Baker, M. J. Optimised Spectral Pre-Processing for Discrimination of Biofluids via ATR-FTIR Spectroscopy. *Analyst.* **2018**, *143*, 6121–6134. DOI: 10.1039/c8an01384e.
9. Hughes, C.; Clemens, G.; Bird, B.; Dawson, T.; Ashton, K. M.; Jenkinson, M. D.; Brodbelt, A.; Weida, M.; Fotheringham, E.; Barre, M.; et al. Introducing Discrete Frequency Infrared Technology for High-Throughput Biofluid Screening. *Sci. Rep.* **2016**, *6*, 20173. DOI: 10.1038/srep20173.
10. Ollesch, J.; Drees, S. L.; Heise, H. M.; Behrens, T.; Brüning, T.; Gerwert, K. FTIR Spectroscopy of Biofluids Revisited: An Automated Approach to Spectral Biomarker Identification. *Analyst.* **2013**, *138*, 4092–4102. DOI: 10.1039/c3an00337j.
11. Goodacre, R.; Baker, M. J.; Graham, D.; Schultz, Z. D.; Diem, M.; Marques, M. P.; Cinque, G.; Vernooij, R.; Sulé-Suso, J.; Byrne, H. J.; et al. Biofluids and Other Techniques: General Discussion. *Faraday Discuss.* **2016**, *187*, 575–601. DOI: 10.1039/C6FD90014C.
12. Algethami, F. K.; Eid, S. M.; Kelani, K. M.; Elghobashy, M. R.; Abd El-Rahman, M. K. Chemical Fingerprinting and Quantitative Monitoring of the Doping Drugs Bambuterol and Terbutaline in Human Urine Samples Using ATR-FTIR Coupled with a PLSR Chemometric Tool. *RSC Adv.* **2020**, *10*, 7146–7154. DOI: 10.1039/c9ra10033d.
13. Berzaghi, P.; Segato, S.; Cozzi, G.; Andrighetto, I. Mid and near Infrared Spectroscopy to Identify Illegal Treatments in Beef Cattle. *Vet. Res. Commun.* **2006**, *30*, 109–112. DOI: 10.1007/s11259-006-0022-z.
14. Rotchell, J. M.; Austin, C.; Chapman, E.; Atherall, C. A.; Liddle, C. R.; Dunstan, T. S.; Blackburn, B.; Mead, A.; Filart, K.; Beeby, E.; et al. Microplastics in Human Urine: Characterisation Using μFTIR and Sampling Challenges Using Healthy Donors and Endometriosis Participants. *Ecotoxicol. Environ. Saf.* **2024**, *274*, 116208. DOI: 10.1016/j.ecoenv.2024.116208.
15. Béjar-Grimalt, J.; Sánchez-Illana, Á.; Guardia, M. d l.; Garrigues, S.; Catalá-Vilaplana, I.; Bermejo-Ruiz, J. L.; Priego-Quesada, J. I.; Pérez-Guaita, D. Dryfilm-ATR-FTIR Analysis of Urinary Profiles as a Point-of-Care Tool to Evaluate Aerobic Exercise. *Anal. Methods.* **2024**, *16*, 5982–5989. DOI: 10.1039/D4AY00913D.
16. Hasni, S.; Khelil, A.; Mahcene, Z.; Bireche, K.; Çebi, N.; Rahmani, Y.; Brahimi, Z.; Ahhmed, A. Physical and Biochemical Characterization of Dromedary Milk as Traditionally Consumed by Bedouins. *Food Chem.* **2023**, *401*, 134191. DOI: 10.1016/j.foodchem.2022.134191.
17. Oliver, K.; Matjiu, F.; Davey, C.; Moochhala, S. H.; Unwin, R.; Rich, P. Attenuated Total Reflection Fourier Transform Infrared (ATR-FTIR) Spectroscopy as a Bedside Diagnostic

Tool for Detecting Renal Disease Biomarkers in Fresh Urine Samples. Proc. SPIE 9332. 2015, 933202, DOI: 10.1117/12.2078971

18. Cerusico, N.; Aybar, J. P.; Lopez, S.; Molina, S. G.; Chavez Jara, R.; Sesto Cabral, M. E.; Valdez, J. C.; Ben Altabef, A.; Ramos, A. N. FTIR Spectroscopy of Chronic Venous Leg Ulcer Exudates: An Approach to Spectral Healing Marker Identification. *Analyst.* **2018**, *143*, 1583–1592. DOI: 10.1039/c7an01909b.
19. Gregório, I.; Zapata, F.; García-Ruiz, C. Analysis of Human Bodily Fluids on Superabsorbent Pads by ATRFTIR. *Talanta.* **2017**, *162*, 634–640. DOI: 10.1016/j.talanta.2016.10.061.
20. Takamura, A.; Watanabe, K.; Akutsu, T.; Ozawa, T. Soft and Robust Identification of Body Fluid Using Fourier Transform Infrared Spectroscopy and Chemometric Strategies for Forensic Analysis. *Sci. Rep.* **2018**, *8*, 8459. DOI: 10.1038/s41598-018-26873-9.
21. Zapata, F.; De La Ossa, M. Á. F.; García-Ruiz, C. Differentiation of Body Fluid Stains on Fabrics Using External Reflection Fourier Transform Infrared Spectroscopy (FT-IR) and Chemometrics. *Appl. Spectrosc.* **2016**, *70*, 654–665. DOI: 10.1177/0003702816631303.
22. Das, T.; Harshey, A.; Srivastava, A.; Nigam, K.; Yadav, V. K.; Sharma, K.; Sharma, A. Analysis of the *Ex-Vivo* Transformation of Semen, Saliva and Urine as They Dry out Using ATRFTIR Spectroscopy and Chemometric Approach. *Sci. Rep.* **2021**, *11*, 11855. DOI: 10.1038/s41598-02191009-5.
23. Sharma, S.; Kaur, H.; Singh, R. Sex Discrimination from Urine Traces for Forensic Purposes Using Attenuated Total Reflectance Fourier Transform Infrared Spectroscopy and Multivariate Data Analysis. *Int. J. Legal Med.* **2022**, *136*, 1755–1765. DOI: 10.1007/s00414-022-02782-5.
24. Abu-Aqil, G.; Sharaha, U.; Suleiman, M.; Riesenberg, K.; Lapidot, I.; Salman, A.; Huleihel, M. Culture-Independent Susceptibility Determination of E. coli Isolated Directly from Patients' Urine Using FTIR and Machine-Learning. *Analyst.* **2022**, *147*, 4815–4823. DOI: 10.1039/d2an01253g.
25. Abu-Aqil, G.; Suleiman, M.; Sharaha, U.; Lapidot, I.; Huleihel, M.; Salman, A. Instant Detection of Extended-Spectrum β-Lactamase-Producing Bacteria from the Urine of Patients Using Infrared Spectroscopy Combined with Machine Learning. *Analyst.* **2023**, *148*, 1130–1140. DOI: 10.1039/d2an01897g.
26. Kotaska, K.; Werle, J.; Hosnedlova, B.; Kizek, R.; Prusa, R. *Use of Fourier Transform Infrared (FTIR) Spectroscopy to Detect Rarely Occurring Cyanoacrylate and Pyrophosphate Urine Stones*; Appl. Spectrosc. Rev.,**2023**.
27. Nsugbe, E.; Ser, H.-L.; Ong, H.-F.; Ming, L. C.; Goh, K.-W.; Goh, B.-H.; Lee, W.-L. On an Affordable Approach towards the Diagnosis and Care for Prostate Cancer Patients Using Urine, FTIR and Prediction Machines. *Diagnostics.* **2022**, *12*, 2099. DOI: 10.3390/diagnostics12092099.
28. Perez-Guaita, D.; Richardson, Z.; Heraud, P.; Wood, B. Quantification and Identification of Microproteinuria Using Ultrafiltration and ATR-FTIR Spectroscopy. *Anal. Chem.* **2020**, *92*, 2409–2416. DOI: 10.1021/acs.analchem.9b03081.
29. Gok, S.; Aydin, O. Z.; Sural, Y. S.; Zorlu, F.; Bayol, U.; Severcan, F. Bladder Cancer Diagnosis from Bladder Wash by Fourier Transform Infrared Spectroscopy as a Novel Test for Tumor Recurrence. *J. Biophotonics.* **2016**, *9*, 967–975. DOI: 10.1002/jbio.201500322.
30. Ortega-Hernández, N.; Ortega-Romero, M.; Medeiros-Domingo, M.; Barbier, O. C.; Rojas-López, M. Detection of Biomarkers Associated with Acute Kidney Injury by a Gold Nanoparticle Based Colloidal Nano-Immunosensor by Fourier-Transform Infrared Spectroscopy with Principal Component Analysis. *Anal. Lett.* **2022**, *55*, 2370–2381. DOI: 10.1080/00032719.2022.2053982.
31. Steenbeke, M.; De Bruyne, S.; Boelens, J.; Oyaert, M.; Glorieux, G.; Van Biesen, W.; Linjala, J.; Delanghe, J. R.; Speeckaert, M. M. Exploring the Possibilities of Infrared Spectroscopy for Urine Sediment Examination and Detection of Pathogenic Bacteria in Urinary Tract Infections. *Clin. Chem. Lab. Med.* **2020**, *58*, 1759–1767. DOI: 10.1515/cclm-2020-0524.

32. Abu-Aqil, G.; Suleiman, M.; Sharaha, U.; Riesenberg, K.; Lapidot, I.; Huleihel, M.; Salman, A. Fast Identification and Susceptibility Determination of E. coli Isolated Directly from Patients' Urine Using Infrared-Spectroscopy and Machine Learning. *Spectrochim. Acta. A Mol. Biomol. Spectrosc.* **2023**, *285*, 121909. DOI: 10.1016/j.saa.2022.121909.
33. Kujdowicz, M.; Mech, B.; Chrabaszcz, K.; Chlosta, P.; Okon, K.; Malek, K. Ftir Spectroscopic Imaging Supports Urine Cytology for Classification of Low-and High-Grade Bladder Carcinoma. *Cancers.* **2021**, *13*, 5734. DOI: 10.3390/cancers13225734.
34. Kujdowicz, M.; Perez-Guaita, D.; Chłosta, P.; Okon, K.; Malek, K. Towards the Point of Care and Noninvasive Classification of Bladder Cancer from Urine Sediment Infrared Spectroscopy. Spectral Differentiation of Normal, Abnormal and Cancer Patients. *Microchem. J.* **2021**, *168*, 106460. DOI: 10.1016/j.microc.2021.106460.
35. Clemens, G.; Hands, J. R.; Dorling, K. M.; Baker, M. J. Vibrational Spectroscopic Methods for Cytology and Cellular Research. *Analyst.* **2014**, *139*, 4411–4444. DOI: 10.1039/c4an00636d.
36. Diem, M.; Miljković, M.; Bird, B.; Mazur, A. I.; Schubert, J. M.; Townsend, D.; Laver, N.; Almond, M.; Old, O. Cancer Screening via Infrared Spectral Cytopathology (SCP): Results for the Upper Respiratory and Digestive Tracts. *Analyst.* **2016**, *141*, 416–428. DOI: 10.1039/c5an01751c.
37. Byrne, H. J.; Knief, P.; Keating, M. E.; Bonnier, F. Spectral Pre and Post Processing for Infrared and Raman Spectroscopy of Biological Tissues and Cells. *Chem. Soc. Rev.* **2016**, *45*, 1865–1878. DOI: 10.1039/c5cs00440c.
38. Li, P.; Williams, R.; Gilbert, S.; Anderson, S. Regulating AI/ML-Enabled Medical Devices in the UK. *ACM Int. Conf. Proceeding Ser.*, **2023**.
39. Office for Product Safety and Standards (OPSS). Study on the Impact of Artificial Intelligence on Product Safety. Commissioned to Centre for Strategy and Evaluation Services (CSES), **2021**. Available at: https://assets.publishing.service.gov.uk/media/628b58e3d3bf7f1f3aa5c13b/impact-of-ai-on-product-safety.pdf.
40. Kurultak, İ.; Sarigul, N.; Kodal, N. S.; Korkmaz, F. Urinalysis of Individuals with Renal Hyperfiltration Using ATR-FTIR Spectroscopy. *Sci. Rep.* **2022**, *12*, 20887. DOI: 10.1038/s41598-022-25535-1.
41. Vayena, E.; Blasimme, A.; Cohen, I. G. Machine Learning in Medicine: Addressing Ethical Challenges. *PLOS Med.* **2018**, *15*, e1002689. DOI: 10.1371/journal.pmed.1002689.
42. Wang, Y.; Fang, L.; Wang, Y.; Xiong, Z. *Current Trends of Raman Spectroscopy in Clinic Settings: Opportunities and Challenges*; Adv. Sci., **2024**.
43. Carvalho, L. F. C. S. *Challenges for Clinical Implementation of Raman and FT-IR Spectroscopy as a Diagnostic Tool*; Photodiagnosis Photodyn Ther., **2020**.
44. Byrne, H. J.; Baranska, M.; Puppels, G. J.; Stone, N.; Wood, B.; Gough, K. M.; Lasch, P.; Heraud, P.; Sulé-Suso, J.; Sockalingum, G. D.; et al. Spectropathology for the Next Generation: Quo Vadis? *Analyst.* **2015**, *140*, 2066–2073. DOI: 10.1039/c4an02036g.
45. Baker, M. J.; Byrne, H. J.; Chalmers, J.; Gardner, P.; Goodacre, R.; Henderson, A.; Kazarian, S. G.; Martin, F. L.; Moger, J.; Stone, N.; et al. Clinical Applications of Infrared and Raman Spectroscopy: State of Play and Future Challenges. *Analyst.* **2018**, *143*, 1735–1757. DOI: 10.1039/c7an01871a.
46. Cameron, J. M.; Rinaldi, C.; Rutherford, S. H.; Sala, A.; Theakstone, A. G.; Baker, M. J. *Clinical Spectroscopy: Lost in Translation?*; Applied Spectroscopy. **2022**.
47. Oudahmane, I.; Sarkees, E.; Taha, F.; Vanmansart, J.; Vuiblet, V.; Larre, S.; Piot, O. To What Extent Does Freezing Impact the Mid-Infrared Signature of Urine? Case of Patients Attending Urology Department. *Spectrochim. Acta. A Mol. Biomol. Spectrosc.* **2024**, *309*, 123820. DOI: 10.1016/j.saa.2023.123820.
48. Oliver, K. V.; Maréchal, A.; Rich, P. R. Effects of the Hydration State on the Mid-Infrared Spectra of Urea and Creatinine in Relation to Urine Analyses. *Appl. Spectrosc.* **2016**, *70*, 983–994. DOI: 10.1177/0003702816641263.
49. Joshi, M.; Deshpande, J. D. Polymerase Chain Reaction: Methods, Principles and Application. www.ssjournals.com.

50. Al-Amrani, S.; Al-Jabri, Z.; Al-Zaabi, A.; Alshekaili, J.; Al-Khabori, M. Proteomics: Concepts and Applications in Human Medicine. *World J. Biol. Chem.* **2021**, *12*, 57–69. DOI: 10.4331/wjbc.v12.i5.57.
51. Pan, S.-W.; Lu, H.-C.; Lo, J.-I.; Ho, L.-I.; Tseng, T.-R.; Ho, M.-L.; Cheng, B.-M. Using an ATR-FTIR Technique to Detect Pathogens in Patients with Urinary Tract Infections: A Pilot Study. *Sensors.* **2022**, *22*, 3638. DOI: 10.3390/s22103638.
52. El-Falouji, A. I.; Sabri, D. M.; Lotfi, N. M.; Medany, D. M.; Mohamed, S. A.; Alaa-Eldin, M.; Selim, A. M.; El Leithy, A. A.; Kalil, H.; El-Tobgy, A.; et al. Rapid Detection of Recurrent Non-Muscle Invasive Bladder Cancer in Urine Using ATR-FTIR Technology. *Molecules.* **2022**, *27*, 8890. DOI: 10.3390/molecules27248890.
53. Farooq, S.; Peres, D. L.; D. C. Caixeta, D. C.; Lima, C.; Da Silva, R. S.; Zezell, D. M. Monitoring Changes in Urine from Diabetic Rats Using ATR-FTIR and Machine Learning. OMN 2023. 2023.
54. Caixeta, D. C.; Lima, C.; Xu, Y.; Guevara-Vega, M.; Espindola, F. S.; Goodacre, R.; Zezell, D. M.; Sabino-Silva, R. Monitoring Glucose Levels in Urine Using FTIR Spectroscopy Combined with Univariate and Multivariate Statistical Methods. *Spectrochim. Acta. A Mol. Biomol. Spectrosc.* **2023**, *290*, 122259. DOI: 10.1016/j.saa.2022.122259.
55. Farooq, S.; Zezell, D. M. Diabetes Monitoring through Urine Analysis Using ATR-FTIR Spectroscopy and Machine Learning. *Chemosensors.* **2023**, *11*, 565. DOI: 10.3390/chemosensors11110565.
56. Miyashita, M.; Ito, N.; Ikeda, S.; Murayama, T.; Oguma, K.; Kimura, J. Development of Urine Glucose Meter Based on Micro-Planer Amperometric Biosensor and Its Clinical Application for Self-Monitoring of Urine Glucose. *Biosens. Bioelectron.* **2009**, *24*, 1336–1340. DOI: 10.1016/j.bios.2008.07.072.
57. Lu, J.; Bu, R. F.; Sun, Z. L.; Lu, Q. S.; Jin, H.; Wang, Y.; Wang, S. H.; Li, L.; Xie, Z. L.; Yang, B. Q.; et al. Comparable Efficacy of Self-Monitoring of Quantitative Urine Glucose with Self-Monitoring of Blood Glucose on Glycaemic Control in Non-Insulin-Treated Type 2 Diabetes. *Diabetes Res. Clin. Pract.* **2011**, *93*, 179–186. DOI: 10.1016/j.diabres.2011.04.012.
58. Dallosso, H. M.; Bodicoat, D. H.; Campbell, M.; Carey, M. E.; Davies, M. J.; Eborall, H. C.; Hadjiconstantinou, M.; Khunti, K.; Speight, J.; Heller, S.; et al. Self-Monitoring of Blood Glucose versus Self-Monitoring of Urine Glucose in Adults with Newly Diagnosed Type 2 Diabetes Receiving Structured Education: A Cluster Randomized Controlled Trial. *Diabet. Med.* **2015**, *32*, 414–422. DOI: 10.1111/dme.12598.
59. Nathan, D. M.; Turgeon, H.; Regan, S. Relationship between Glycated Haemoglobin Levels and Mean Glucose Levels over Time. *Diabetologia.* **2007**, *50*, 2239–2244. DOI: 10.1007/s00125007-0803-0.
60. Thornton-Swan, T. D.; Armitage, L. C.; Curtis, A. M.; Farmer, A. J. *Assessment of Glycaemic Status in Adult Hospital Patients for the Detection of Undiagnosed Diabetes Mellitus: A Systematic Review*; Diabet Med., **2022**.
61. Lin, H.; Wang, Z.; Luo, Y.; Lin, Z.; Hong, G.; Deng, K.; Huang, P.; Shen, Y. Non/Mini-Invasive Monitoring of Diabetes-Induced Myocardial Damage by Fourier Transform Infrared Spectroscopy: Evidence from Biofluids. *Biochim. Biophys. Acta. Mol. Basis Dis.* **2022**, *1868*, 166445. DOI: 10.1016/j.bbadis.2022.166445.
62. Richardson, Z.; Kincses, A.; Ekinci, E.; Perez-Guaita, D.; Jandeleit-Dahm, K.; Wood, B. R. ATR-FTIR Spectroscopy for Early Detection of Diabetic Kidney Disease. *Analysis and Sensing* **2023**, *3, 1-9*. DOI: 10.1002/anse.202200094.
63. Primiano, A.; Persichilli, S.; Di Giacinto, F.; Ciasca, G.; Baroni, S.; Ferraro, P. M.; De Spirito, M.; Urbani, A.; Gervasoni, J. Attenuated Total reflection-Fourier Transform Infrared Spectroscopy (ATR-FTIR) Detection as a Rapid and Convenient Screening Test for Cystinuria. *Clin. Chim. Acta.* **2021**, *518*, 128–133. DOI: 10.1016/j.cca.2021.03.017.
64. Buhas, B. A.; Muntean, L. A.-M.; Ploussard, G.; Feciche, B. O.; Andras, I.; Toma, V.; Maghiar, T. A.; Crișan, N.; Știufiuc, R.-I.; Lucaciu, C. M.; et al. Renal Cell Carcinoma Discrimination through Attenuated Total Reflection Fourier Transform Infrared

Spectroscopy of Dried Human Urine and Machine Learning Techniques. *Int. J. Mol. Sci.* **2024**, *25*, 9830. DOI: 10.3390/ijms25189830.

65. Tian, Y.; Fan, X.; Chen, K.; Chen, X.; Peng, W.; Wang, L.; Wang, F. Optical Biomarker Analysis for Renal Cell Carcinoma Obtained from Preoperative and Postoperative Patients Using ATR-FTIR Spectroscopy. *Spectrochim. Acta. A Mol. Biomol. Spectrosc.* **2024**, *318*, 124426. DOI: 10.1016/j.saa.2024.124426.
66. Duckworth, E.; Mortimer, M.; Al-Sarireh, B.; Kanamarlapudi, V.; Roy, D. Frontline Clinical Diagnosis—FTIR on Pancreatic Cancer. *Cancer Med.* **2023**, *12*, 17340–17345. DOI: 10.1002/cam4.6346.
67. Bassan, P.; Sachdeva, A.; Kohler, A.; Hughes, C.; Henderson, A.; Boyle, J.; Shanks, J. H.; Brown, M.; Clarke, N. W.; Gardner, P.; et al. FTIR Microscopy of Biological Cells and Tissue: Data Analysis Using Resonant Mie Scattering (RMieS) EMSC Algorithm. *Analyst.* **2012**, *137*, 1370–1377. DOI: 10.1039/c2an16088a.
68. Paraskevaidi, M.; Morais, C. L. M.; Lima, K. M. G.; Ashton, K. M.; Stringfellow, H. F.; Martin-Hirsch, P. L.; Martin, F. L. Potential of Mid-Infrared Spectroscopy as a Non-Invasive Diagnostic Test in Urine for Endometrial or Ovarian Cancer. *Analyst.* **2018**, *143*, 3156–3163. DOI: 10.1039/c8an00027a.
69. Giamougiannis, P.; Morais, C. L. M.; Rodriguez, B.; Wood, N. J.; Martin-Hirsch, P. L.; Martin, F. L. Detection of Ovarian Cancer (± Neo-Adjuvant Chemotherapy Effects) via ATR-FTIR Spectroscopy: Comparative Analysis of Blood and Urine Biofluids in a Large Patient Cohort. *Anal. Bioanal. Chem.* **2021**, *413*, 5095–5107. DOI: 10.1007/s00216-021-03472-8/Published.
70. Ramirez, C. A. M.; Stringfellow, H.; Naik, R.; Crosbie, E. J.; Paraskevaidi, M.; Rehman, I. U.; Martin-Hirsch, P. Infrared Spectroscopy of Urine for the Non-Invasive Detection of Endometrial Cancer. *Cancers.* **2022**, *14*, 1–16.DOI: 10.3390/cancers14205015.
71. Paraskevaidi, M.; et al. *Clinical Applications of Infrared and Raman Spectroscopy in the Fields of Cancer and Infectious Diseases*; Appl. Spectrosc. Rev., **2021**.
72. Maitra, I.; Morais, C. L. M.; Lima, K. M. G.; Ashton, K. M.; Date, R. S.; Martin, F. L. Attenuated Total Reflection Fourier-Transform Infrared Spectral Discrimination in Human Bodily Fluids of Oesophageal Transformation to Adenocarcinoma. *Analyst.* **2019**, *144*, 7447–7456. DOI: 10.1039/c9an01749f.
73. Barr, D. B.; Wilder, L. C.; Caudill, S. P.; Gonzalez, A. J.; Needham, L. L.; Pirkle, J. L. Urinary Creatinine Concentrations in the U.S. population: Implications for Urinary Biologic Monitoring Measurements. *Environ. Health Perspect.* **2005**, *113*, 192–200. DOI: 10.1289/ehp.7337.
74. Robinson-Cohen, C.; Ix, J. H.; Smits, G.; Persky, M.; Chertow, G. M.; Block, G. A.; Kestenbaum, B. R. Estimation of 24-Hour Urine Phosphate Excretion From Spot Urine Collection: Development of a Predictive Equation. *J. Ren. Nutr.* **2014**, *24*, 194–199. DOI: 10.1053/j.jrn.2014.02.001.
75. Werle, J.; Buresova, K.; Cepova, J.; Bjørklund, G.; Fortova, M.; Prusa, R.; Fernandez, C.; Dunovska, K.; Klapkova, E.; Kizek, R.; et al. Spectrophotometric and Chromatographic Analysis of Creatine: Creatinine Crystals in Urine. *Spectrochim. Acta. A Mol. Biomol. Spectrosc.* **2024**, *322*, 124689. DOI: 10.1016/j.saa.2024.124689.
76. Aitekenov, S.; Gaipov, A.; Bukasov, R. *Review: Detection and Quantification of Proteins in Human Urine*; Talanta., **2021**.
77. Sarigul, N.; Korkmaz, F.; Kurultak, İ. A New Artificial Urine Protocol to Better Imitate Human Urine. *Sci. Rep.* **2019**, *9*, 20159. DOI: 10.1038/s41598-019-56693-4.
78. Sarigul, N.; Bozatli, L.; Kurultak, I.; Korkmaz, F. Using Urine FTIR Spectra to Screen Autism Spectrum Disorder. *Sci. Rep.* **2023**, *13*, 19466. DOI: 10.1038/s41598-023-46507-z.
79. Sarigul, N.; Kurultak, İ.; Uslu Gökceoğlu, A.; Korkmaz, F. Urine Analysis Using FTIR Spectroscopy: A Study on Healthy Adults and Children. *J. Biophotonics.* **2021**, *14*, e202100009. DOI: 10.1002/jbio.202100009.

80. Pradhane, A. P.; Methekar, R. N.; Agrawal, S. G. Investigations on Melamine-Based Uric Acid Kidney Stone Formation and Its Prevention by Inhibitors. *Urolithiasis.* **2023**, *51*, 68. DOI: 10.1007/s00240-02301437-3.
81. Rathore, A. S.; Roy, D. Performance of LDA and DCT Models. *J. Inf. Sci.* **2014**, *40*, 281–292. DOI: 10.1177/0165551514524678.
82. Thomas, C. E.; Sexton, W.; Benson, K.; Sutphen, R.; Koomen, J. Urine Collection and Processing for Protein Biomarker Discovery and Quantification. Cancer Epidemiol Biomarkers Prev. **2010**, 4, 953-959. DOI: 10.1158/1055-9965.EPI-10-0069.
83. Li, Z.; Romanoff, L. C.; Lewin, M. D.; Porter, E. N.; Trinidad, D. A.; Needham, L. L.; Patterson, D. G.; Sjödin, A. Variability of Urinary Concentrations of Polycyclic Aromatic Hydrocarbon Metabolite in General Population and Comparison of Spot, First-Morning, and 24-h Void Sampling. *J. Expo. Sci. Environ. Epidemiol.* **2010**, *20*, 526–535. DOI: 10.1038/jes.2009.41.
84. Zhang, T.; Chang, X.; Liu, W.; Li, X.; Wang, F.; Huang, L.; Liao, S.; Liu, X.; Zhang, Y.; Zhao, Y.; et al. Comparison of Sodium, Potassium, Calcium, Magnesium, Zinc, Copper and Iron Concentrations of Elements in 24-h Urine and Spot Urine in Hypertensive Patients with Healthy Renal Function. *J. Trace Elem. Med. Biol.* **2017**, *44*, 104–108. DOI: 10.1016/j.jtemb.2017.06.006.
85. Ristenpart, W. D.; Kim, P. G.; Domingues, C.; Wan, J.; Stone, H. A. Influence of Substrate Conductivity on Circulation Reversal in Evaporating Drops. *Phys. Rev. Lett.* **2007**, *99*, 234502. DOI: 10.1103/PhysRevLett.99.234502.
86. Yunker, P. J.; Still, T.; Lohr, M. A.; Yodh, A. G. Suppression of the Coffee-Ring Effect by Shape-Dependent Capillary Interactions. *Nature.* **2011**, *476*, 308–311. DOI: 10.1038/nature10344.
87. Cameron, J. M.; Butler, H. J.; Palmer, D. S.; Baker, M. J. *Biofluid Spectroscopic Disease Diagnostics: A Review on the Processes and Spectral Impact of Drying*; J. Biophotonics., **2018**.
88. Mampallil, D.; Eral, H. B. *A Review on Suppression and Utilization of the Coffee-Ring Effect*; Adv. Colloid Interface Sci., **2018**, 252, 38–54.
89. Esmonde-White, K. A.; Esmonde-White, F. W. L.; Morris, M. D.; Roessler, B. J. Characterization of Biofluids Prepared by Sessile Drop Formation. *Analyst.* **2014**, *139*, 2734–2741. DOI: 10.1039/c3an02175k.
90. Lovergne, L.; Clemens, G.; Untereiner, V.; Lukaszweski, R. A.; Sockalingum, G. D.; Baker, M. J. Investigating Optimum Sample Preparation for Infrared Spectroscopic Serum Diagnostics. *Anal. Methods.* **2015**, *7*, 7140–7149. DOI: 10.1039/c5ay00502g.
91. Xie, Y.; Huang, Y.; Wang, W.; Liu, G.; Zhao, R. Dynamic Interaction between Melamine and Cyanuric Acid in Artificial Urine Investigated by Quartz Crystal Microbalance. *Analyst.* **2011**, *136*, 2482–2488. DOI: 10.1039/c1an15119c.
92. Stumpe, M. C.; Grubmüller, H. Aqueous Urea Solutions: Structure, Energetics, and Urea Aggregation. *J. Phys. Chem. B.* **2007**, *111*, 6220–6228. DOI: 10.1021/jp066474n.
93. Rezus, Y. L. A.; Bakker, H. J. Effect of Urea on the Structural Dynamics of Water, **2006**. www.pnas.orgcgidoi10.1073pnas.0606538103.
94. Hoşafçı, G.; Klein, O.; Oremek, G.; Mäntele, W. Clinical Chemistry without Reagents? An Infrared Spectroscopic Technique for Determination of Clinically Relevant Constituents of Body Fluids. *Anal. Bioanal. Chem.* **2007**, pp. 1815–1822.
95. Furlan, P.; Servey, J.; Scott, S.; Peaslee, M. FTIR Analysis of Mouse Urine Urea Using IR Cards. *Spectrosc. Lett.* **2004**, *37*, 311–318. DOI: 10.1081/SL-120038766.
96. Farhan, M. A.; Al-Garawi, Z. S.; Ali, W. B.; Nief, O. A. A Novel Method for Long-Term Preserving of Urine Microstructure Using Poly(Vinyl Chloride). *J. Appl. Polym. Sci.* **2023**, *140*. DOI: 10.1002/app.54000.
97. Yu, M.-C.; Rich, P.; Foreman, L.; Smith, J.; Yu, M.-S.; Tanna, A.; Dibbur, V.; Unwin, R.; Tam, F. W. K. Label Free Detection of Sensitive Mid-Infrared Biomarkers of Glomerulonephritis in Urine Using Fourier Transform Infrared Spectroscopy. *Sci. Rep.* **2017**, *7*, 4601. DOI: 10.1038/s41598-01704774-7.